

# IMPROVEMENTS IN A MULTI-REFLECTING TOF MASS SPECTROMETER TO ENHANCE MASS SPECTROMETRY IMAGING SPECIFICITY

Emmanuelle Claude<sup>1</sup>; William Johnson<sup>1</sup>; Joel Keelor<sup>2</sup>; Emma Marsden-Edwards<sup>1</sup>; Martin Palmer<sup>1</sup>  
<sup>1</sup>Waters Corporation, Wilmslow, United Kingdom; <sup>2</sup>Waters Corporation, Milford, MA

## INTRODUCTION

Mass spectrometry imaging (MSI) provides a method to visualize the spatial distribution of molecules across a surface, with MALDI and DESI being the most common techniques used.

The complexity of MSI data can make accurate identification of analytes a challenge due to overlapping species. Therefore, it is desirable to acquire data at the highest mass spectral resolving power possible to reduce interference. However, MSI experiments that use high spatial resolution often require long acquisition times and can be further limited by the scan speed of the mass spectrometer. Here we employ a method of extending the flight path to enable a second pass of an Multi Reflecting Time of Flight (MRT) analyzer that increases the resolving power by >50% enabling >300,000 FWHM.

## METHODS

The SELECT SERIES™ MRT is a hybrid q-ToF mass spectrometer that employs a multi-reflecting time of flight analyzer<sup>1</sup>. The analyzer has a theoretically unlimited mass range as the ions travel a fixed pathlength from the orthogonal accelerator to the detector, the observed resolving power, R (being defined as R = pathlength/2x time spread), increases with an increased pathlength, this can be achieved by making the analyzer physically longer or by deflecting the ions within the analyzer and enabling them to make multiple passes of the device. The former has practical physical limitations whereas the later can be achieved by applying a timed pulse to an electrode deflecting the ions within the device. Figure 1 shows the ion path of the MRT operating in a standard single pass mode, the ions enter the analyzer through a orthogonal accelerator and follow a trajectory between lenses P1 and P23 shown in blue, once the ions reach lens P23 they are deflected back in a trajectory towards P1, shown in red, and the detector, resulting in a pathlength of ~47m and a resolving power of ~200,000 FWHM, this mode of operation is called Multi-Reflecting ToF (MRT) mode.

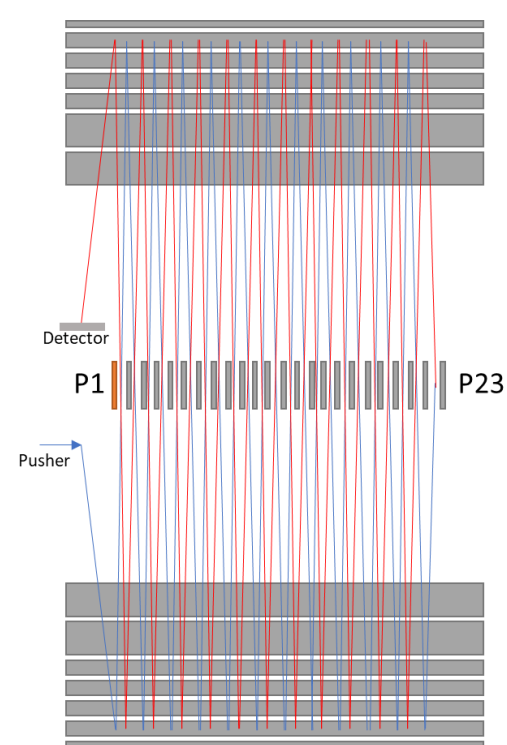


Figure 1. Flight path of MRT operating in a standard single pass mode.

The analyzer can also be operated with a timed pulse applied to lens P1, deflecting a restricted mass range so as to undergo two passes, increasing the pathlength and hence observed resolving power to ~300,000 FWHM. This is shown in Figure 2, the ions enter the analyzer through a orthogonal accelerator and follow a trajectory between lenses P1 and P23 shown in blue (Fig 2A), once the ions reach lens P23 they are deflected back in a trajectory towards P1, shown in red (Fig 2B), a timed pulse is then applied to lens P1 (shown in orange) deflecting the ions back towards P23 (Fig 2C) shown in green, once the ions reach lens P23 they are deflected back again in a trajectory, shown in yellow, towards P1 and finally the detector (Fig 2D), resulting in a pathlength of ~92m and a resolving power of ~300,000 FWHM.

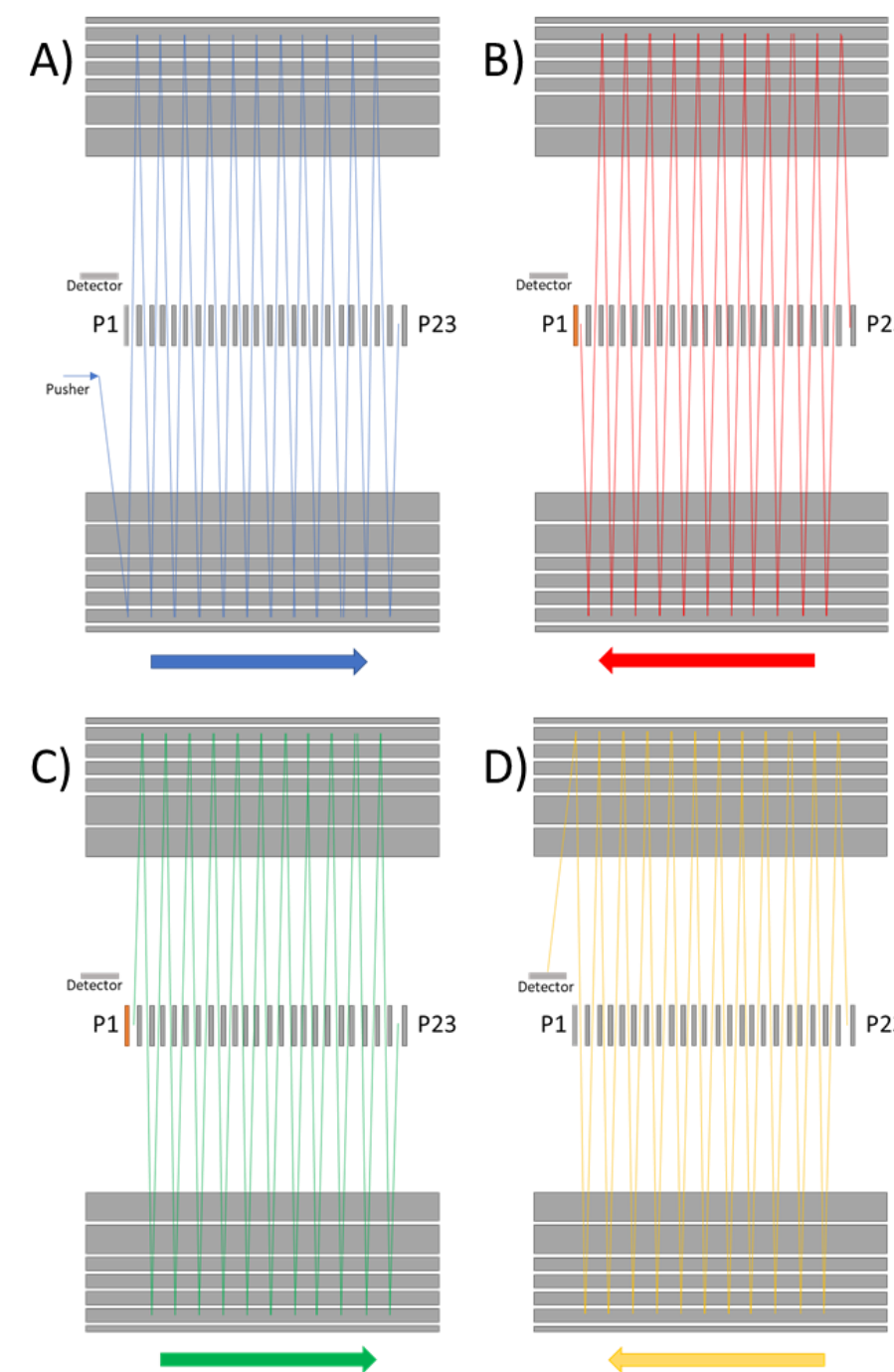


Figure 2. Flight path of MRT analyzer operating in a Resolution Enhancement Mode (REM), double pass mode, A: ions pass (shown in blue) from orthogonal accelerator into analyzer and are focussed and reflected towards lens P23; B: ions are deflected by lens P23 back towards lens P1, shown in red; C: a timed pulse applied to P1 deflects the ions back towards lens P23, shown in green; D: ions are deflected a second time by lens P23 back towards P1 (pulse off) and onto the detector (shown in yellow).

The transmittable mass range is a function of the selected low  $m/z$ , with the high  $m/z$  limit being approximately four times that of the lowest  $m/z$ , so for a start mass of  $m/z$  300 the upper  $m/z$  would be ~1100  $m/z$ .

Another consideration of the described approach to increase pathlength is a decrease in duty cycle, this is overcome through a synchronization of the time of flight of an ion packet release between the upstream gas cell and the orthogonal accelerator for the  $m/z$  range of interest. This mode of operation is called Resolution Enhancement Mode (REM).

## EXPERIMENTAL

A healthy wild-type mouse kidney and brain were axially cryo-sectioned onto standard glass slides at a thickness of 16  $\mu\text{m}$ . The sections were analysed on a DESI XS source fitted to a SELECT SERIES MRT in duplicate employing either a single or double pass of the analyzer. DESI spray conditions were set at 2  $\mu\text{L}/\text{min}$ , 95:5 MeOH: water with 100  $\text{pg}/\mu\text{L}$  Leu-enkephalin with 0.86 kV and 15 psi nebulising gas applied to the DESI High Performance Sprayer, the Heated Transfer Line was maintained at 350°C. Acquisitions were performed in full scan MS at two spectra per second for positive ionisation mode. Data were processed using High Definition™ Imaging (HDI v1.7) imaging software to generate segmentation and analyte identification for the different regions of the brain (namely cortex, hippocampus and cerebellum) and kidney (cortex and medulla).

## RESULTS

Firstly consecutive tissue sections were analyzed in standard MRT mode with a MS resolution of ~200,000 FWHM and in MRT-REM mode with an MS resolution of ~300,000 FWHM.

Figure 3 demonstrates the improvement observed with increased MS resolving power with baseline resolution of four peaks within a 30mDa window around  $m/z$  850.56. Putative identification using LipidMaps database gave two isotopic peaks from the fine isotope structure <sup>13</sup>C and <sup>41</sup>K of lipid PC(38:4), generating the same ion images. The other peaks were identified as potassiumated PC(38:3) and an ammonia adduct of TG(48:11;O3).

When mass difference between molecules is less than 5 mDa, an MS resolution of >200,000 FWHM is required to distinguish localization as illustrated in Figure 4. Sodiated PC (34:1) and protonated PC (36:4) lipids have a difference  $m/z$  of 2.4 mDa and have different localization in mouse kidney, whereas with an MS resolution 200,000 FWHM, it wasn't possible to differentiate them.

MRT routinely provides sub ppm mass accuracy, tentative identification of a selection of lipids observed in the kidney section are displayed in Table 1, showing an overall RMS mass error of 74 ppb.

Tentative ID	Formula	Adduct	Expected mass	Observed mass	mDa error	ppb error
SM (34:1)	C <sub>39</sub> H <sub>79</sub> N <sub>2</sub> O <sub>6</sub> P	Na <sup>+</sup>	725.55680	725.55676	-0.040	-55
SM (34:1;O2)	C <sub>39</sub> H <sub>79</sub> N <sub>2</sub> O <sub>6</sub> P	K <sup>+</sup>	741.53073	741.5307	-0.030	-40
PC (34:2)	C <sub>42</sub> H <sub>80</sub> NO <sub>8</sub> P	H <sup>+</sup>	758.56943	758.5694	-0.031	-41
PC (34:1)	C <sub>42</sub> H <sub>82</sub> NO <sub>8</sub> P	H <sup>+</sup>	760.58508	760.58508	-0.002	-2
PC (32:0)	C <sub>40</sub> H <sub>80</sub> NO <sub>8</sub> P	K <sup>+</sup>	772.52531	772.52521	-0.103	-133
PC (34:2)	C <sub>42</sub> H <sub>80</sub> NO <sub>8</sub> P	Na <sup>+</sup>	780.55138	780.55145	0.074	95
PC (36:2)	C <sub>44</sub> H <sub>84</sub> NO <sub>8</sub> P	H <sup>+</sup>	786.60073	786.60077	0.038	49
PC (34:2)	C <sub>42</sub> H <sub>80</sub> NO <sub>8</sub> P	K <sup>+</sup>	796.52531	796.52533	0.017	21
PC (36:4)	C <sub>44</sub> H <sub>80</sub> NO <sub>8</sub> P	Na <sup>+</sup>	804.55138	804.55133	-0.046	-57
PC (36:4)	C <sub>44</sub> H <sub>80</sub> NO <sub>8</sub> P	K <sup>+</sup>	820.52531	820.52527	-0.043	-53
PC (36:3)	C <sub>44</sub> H <sub>82</sub> NO <sub>8</sub> P	K <sup>+</sup>	822.54096	822.54089	-0.073	-89
PC (36:2)	C <sub>44</sub> H <sub>84</sub> NO <sub>8</sub> P	K <sup>+</sup>	824.55661	824.55664	0.027	32
PC (38:4)	C <sub>46</sub> H <sub>84</sub> NO <sub>8</sub> P	Na <sup>+</sup>	832.58268	832.58276	0.084	101
PC (38:6)	C <sub>46</sub> H <sub>80</sub> NO <sub>8</sub> P	K <sup>+</sup>	844.52531	844.52527	-0.040	-47
PC (38:5)	C <sub>46</sub> H <sub>82</sub> NO <sub>8</sub> P	K <sup>+</sup>	846.54096	846.54095	-0.013	-16
PC (38:4)	C <sub>46</sub> H <sub>84</sub> NO <sub>8</sub> P	K <sup>+</sup>	848.55661	848.55658	-0.033	-39
PC (O-40:7)	C <sub>48</sub> H <sub>84</sub> NO <sub>7</sub> P	K <sup>+</sup>	856.56170	856.56177	0.070	82
PC (40:6)	C <sub>48</sub> H <sub>84</sub> NO <sub>8</sub> PK	K <sup>+</sup>	872.55661	872.55658	-0.030	-34
SM( 44:4;O5)	C <sub>49</sub> H <sub>93</sub> N <sub>2</sub> O <sub>6</sub> P	H <sup>+</sup>	885.66915	885.66907	-0.080	-90
SM (46:6O5)	C <sub>51</sub> H <sub>93</sub> N <sub>2</sub> O <sub>6</sub> P	H <sup>+</sup>	909.66915	909.66901	-0.140	-154
				RMS	0.057	74

Table 1 Observed mass accuracy for selected lipids observed in kidney section data

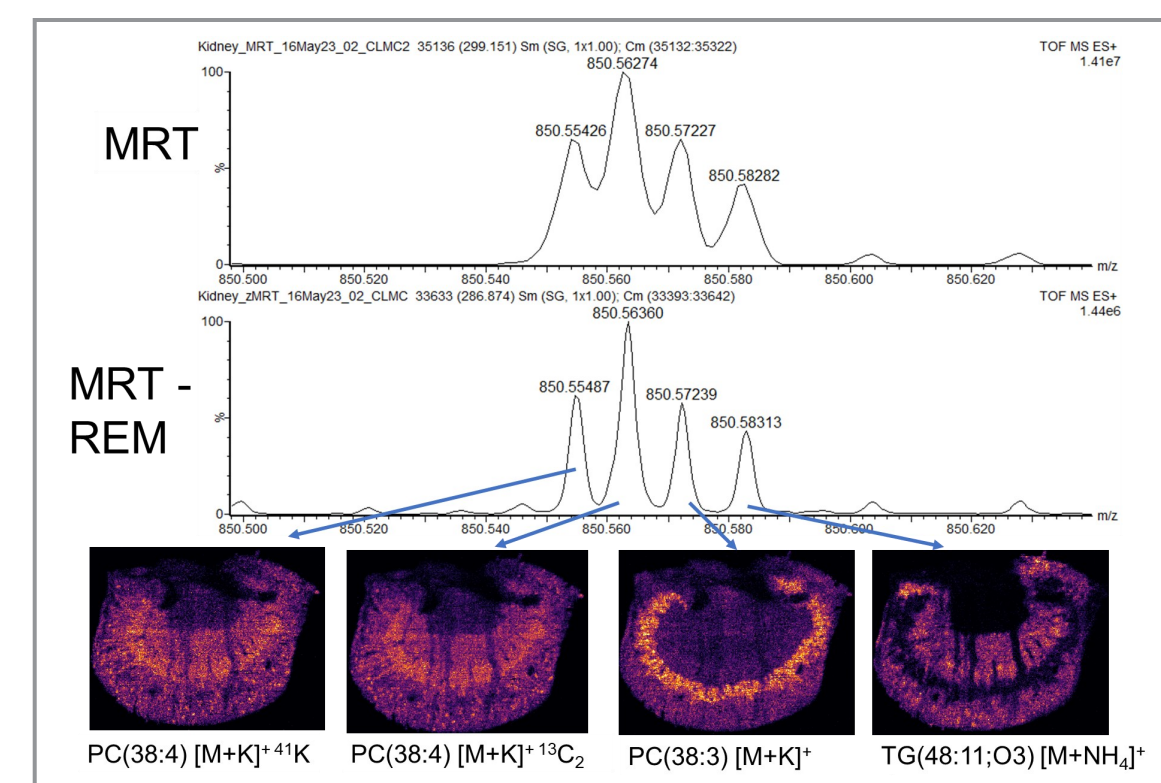


Figure 3 MRT vs. MRT-REM MS spectra acquired from mouse kidney tissue section ~m/z 850.56 showing MS resolution improvement at 300,000 FWHM with baseline peak separation.

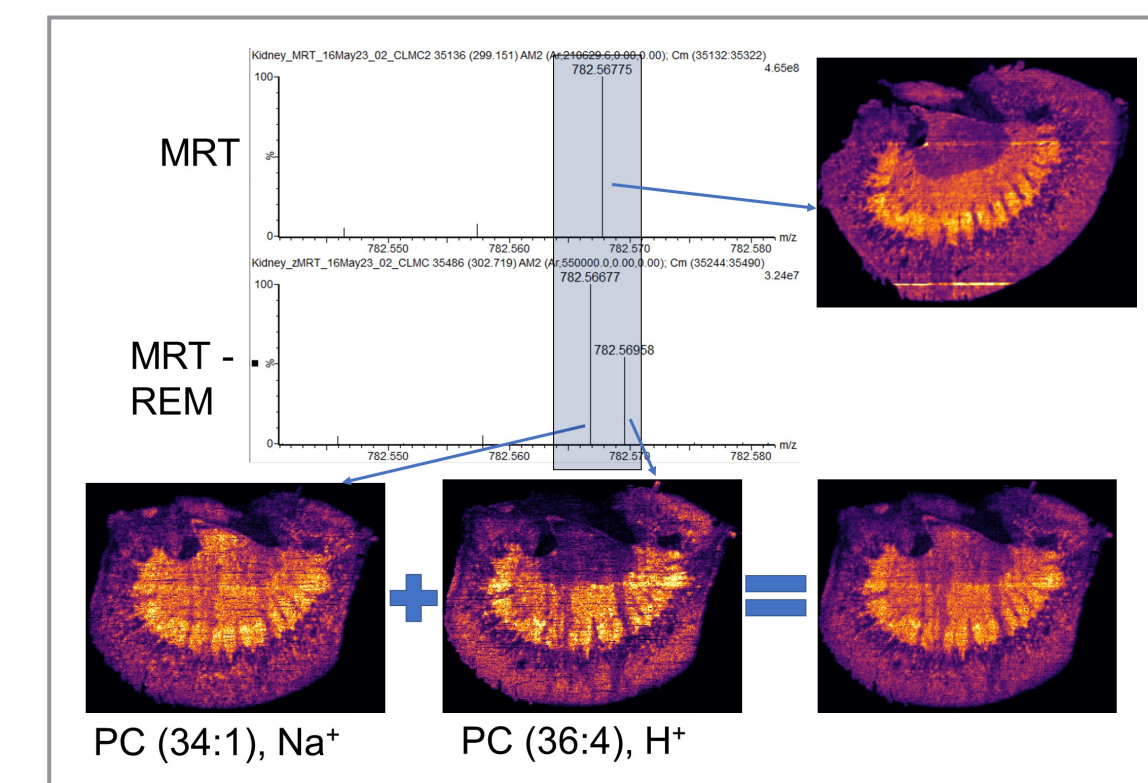


Figure 4 MRT vs. MRT-REM MS spectra acquired from mouse kidney tissue section ~m/z 782.57 showing different localization of sodiated PC (34:1) and protonated PC (36:4) which are less than 3mDa difference in  $m/z$  when sample was analysed in MRT-REM mode at 300,000 FWHM MS resolution.

A further example is presented in Figure 5 where consecutive mouse brain tissue sections were analyzed in both modes of operation, it was observed that two molecules had a mass difference of 2.8 mDa. In the MRT-REM MS spectrum in Figure 5B the peaks are not baseline resolved, however, when the MS imaging data are processed with a mass window of 1 mDa, it was possible to differentiate two specific distributions, one which was ubiquitous and one specific to certain tissue types.

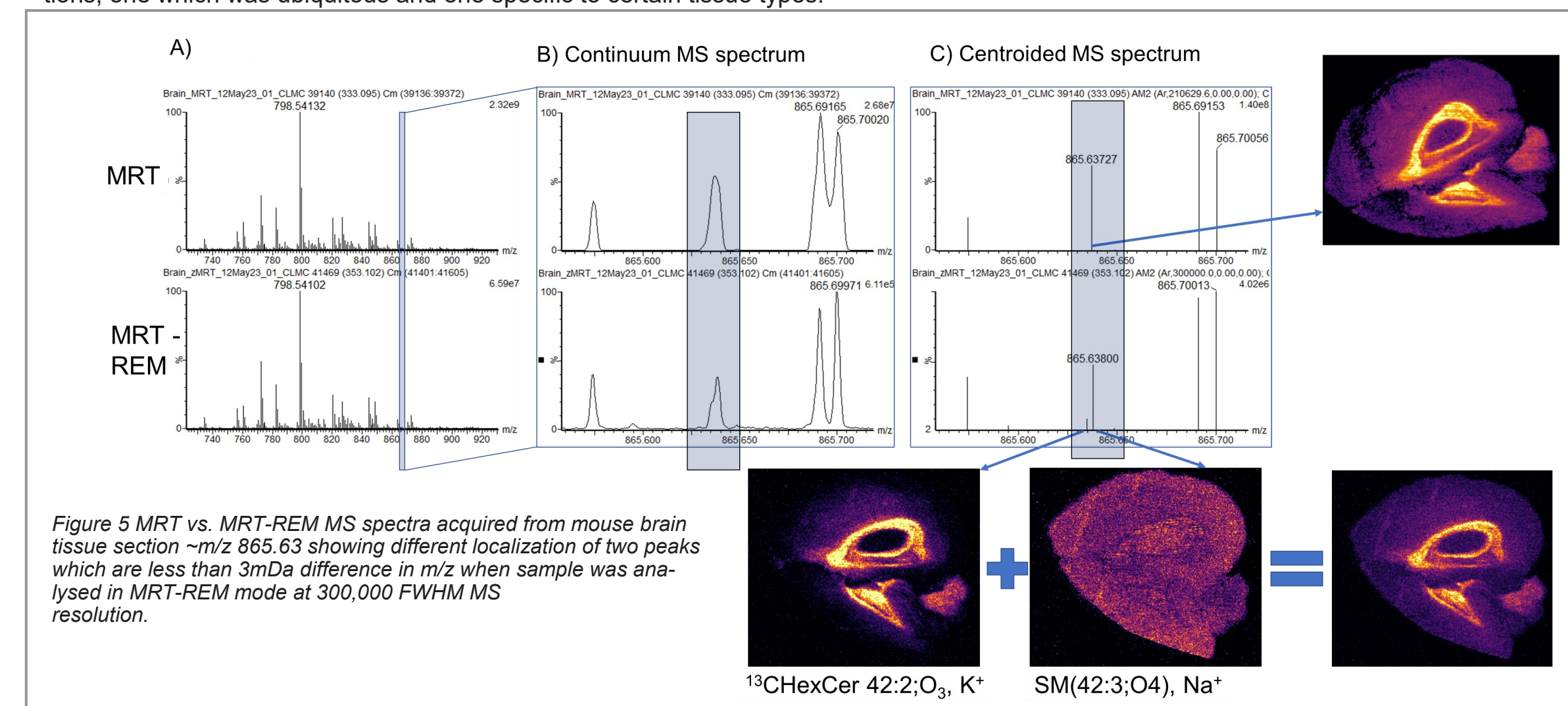


Figure 5 MRT vs. MRT-REM MS spectra acquired from mouse brain tissue section ~m/z 865.63 showing different localization of two peaks which are less than 3mDa difference in  $m/z$  when sample was analysed in MRT-REM mode at 300,000 FWHM MS resolution.

## CONCLUSION

- A novel approach to increasing mass resolving power on a multi-reflecting ToF allowing an improvement of imaging clarity has been presented.
- Multiple examples of ions that were previously unresolved can now be separated resulting in increased imaging specificity, for example, four ions within a 30mDa window were baseline resolving allowing putative identification to be made and images free from interferences.
- Excellent mass accuracy, 74 ppb RMS, is observed for a selection of lipids present in the murine kidney section.

## REFERENCES

- Novel Hybrid Quadrupole-Multireflecting Time-of-Flight Mass Spectrometry System, DA Cooper-Shepherd et al. J. Am. Soc. Mass Spectrometry 2023 34 (2), 264-272. DOI: 10.1021/jasms.2c00281